THE JOURNAL OF PHYSICAL CHEMISTRY C

Article

Cite This: J. Phys. Chem. C 2019, 123, 12376−12381

pubs.acs.org/JPCC

Interaction of Gold with Oxide Nanoparticles: Size or Electronic Effect?

Published as part of The Journal of Physical Chemistry virtual special issue "Hai-Lung Dai Festschrift".

Oleksandr Bondarchuk,[#] Shamil Shaikhutdinov,[*] and Hans-Joachim Freund

Abteilung Chemische Physik, Fritz-Haber-Institut der Max-Planck-Gesellschaft, Faradayweg 4-614195, Berlin

Supporting Information

ABSTRACT: We have studied the interaction of gold with highly dispersed silica particles and flat silica films using scanning tunneling microscopy, X-ray photoelectron spectroscopy, and infrared spectroscopy. The results revealed the definitive role of the oxide morphology on the electronic structure, thermal stability, and CO adsorption capabilities of gold species formed. Comparison with our previous study of gold supported on ceria nanoparticles and films suggests that it is the nanoparticulate morphology of the oxide support rather than its reducibility that promotes the formation and stabilization of partially charged $Au^{\delta+}$ species.

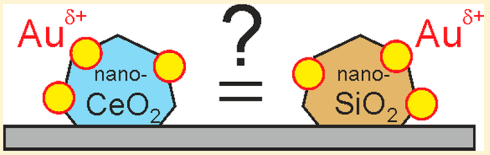

1. INTRODUCTION

Gold has long been considered to be chemically inert material. It has only rather recently been recognized that highly dispersed gold supported on oxides exhibits high activity in a number of chemical reactions.[1] This somewhat unexpected property of Au nanoparticles stimulated an enormous number of studies in catalysis, photonics, and biology.[2,3] In spite of the great interest and enhanced activities worldwide, the reaction mechanisms which are based on detailed knowledge about the atomic structure and electronic properties of supported gold species are still far from being well understood. For sustained catalytic activity, a long-term stability of a "nano-gold" is critical. This is particularly important for the so-called "single-atom catalysis"[4] that has recently received much attention as an ultimate limit of metal dispersion in oxide-supported catalysts. However, gold sintering, either on heating or induced by the reaction atmosphere, remains an issue.

Reducible oxide supports such as TiO_2 and CeO_2 are often used for gold catalysts. It is commonly believed that reducible oxides aid in the formation of active gold species via the strong interaction with the oxide surface leading to charge transfer. In our own laboratories, we have recently shown that CeO_2 nanoparticles ("nanoceria") stabilize gold species exhibiting electronic and adsorption characteristics of partially oxidized $Au^{\delta+}$.[5] In contrast, gold vapor-deposited onto defect-free $CeO_2(111)$ films only showed metallic gold. The difference could be the reason for superior activity observed on Au/nanoceria catalysts in the CO oxidation reaction as compared to conventional Au/CeO_2 catalysts.[6]

The observation of positively charged gold on nanoceria is puzzling as evidence has shown that gold atoms charge negatively on reduced, defected CeO_{2-x} and are neutral on perfectly stoichiometric CeO_2.[7] Positively charged Au has been observed, for example, on an FeO(111) monolayer film grown on Pt(111) and may be traced back to the high work function of the support which leads to a preferential transfer of electrons from Au to the FeO/Pt interface[8] in contrast to Au deposited on ultrathin MgO(001) films on Ag(001) where the charge transfer occurs in the opposite direction.[9] Another possibility to drive electrons from adsorbed Au into the oxide support is a higher oxygen loading of the support (or cation deficiency)[10] or specific edge sites on stoichiometric oxide films.[11] It is therefore of importance to compare the results on nanoceria with another system of oxide nanoparticles on the same substrate. In this paper, we show that silica nanoparticles ("nanosilica") lead to a similar formation of $Au^{\delta+}$ species indicating that one of the above mechanisms is, indeed, active.

2. METHODS

The experiments were carried out in an ultrahigh vacuum (UHV) chamber (base pressure 5×10^{-10} mbar) equipped with scanning tunneling microscopy (STM, from Omicron), X-ray photoelectron spectroscopy (XPS, Scienta SES 200 analyzer), and infrared reflection−absorption spectroscopy (IRAS, Bruker IFS 66v/s).

XP spectra were recorded using an X-ray source (Mg K_α radiation, $h\nu$ = 1253.6 eV) from SPECS. The spectrometer was calibrated by setting the Au $4f_{7/2}$ level, measured on a gold foil attached to the sample stage on the manipulator, to 84.0 eV. IRA spectra with 4 cm^{-1} resolution were measured at 8° grazing incidence in a specular geometry. The STM images were acquired in constant current mode using W tips at the tunneling current of 0.1−0.2 nA and sample bias of 1.5−2.5 V.

Silicon (99.99%, Goodfellow) was deposited from a rod of 2 mm in diameter, while gold (99.9% Goodfellow) was deposited using a crucible, both installed in an electron

Received: March 19, 2019
Revised: April 29, 2019
Published: April 29, 2019

beam assisted evaporator (Omicron EFM3). During evaporation the sample was biased to the same potential as the target source to prevent accelerating of the charged species toward the sample.

Silica nanoparticles were prepared on top of a "monolayer" silica film, which was in turn grown on a Mo(112) substrate as described in detail elsewhere.[12,13] The silica films were inspected by STM, XPS, and IRAS prior to the silica particle deposition. In addition, XP spectra of the films were used for calibration of the Si source, henceforth presented in monolayers equivalent to prepare monolayer silica film (MLE). Silica nanoparticles formed by Si vapor deposition in 10^{-6} mbar of O_2 at either 100 or 300 K and subsequent annealing at 600 K in oxygen for 10 min. The amount of gold was calibrated via STM and XPS of the Au deposited onto a pure silica film.

3. RESULTS AND DISCUSSION

Figure 1a displays a typical STM image of a crystalline silica film used as support for the silica nanoparticles (NPs).

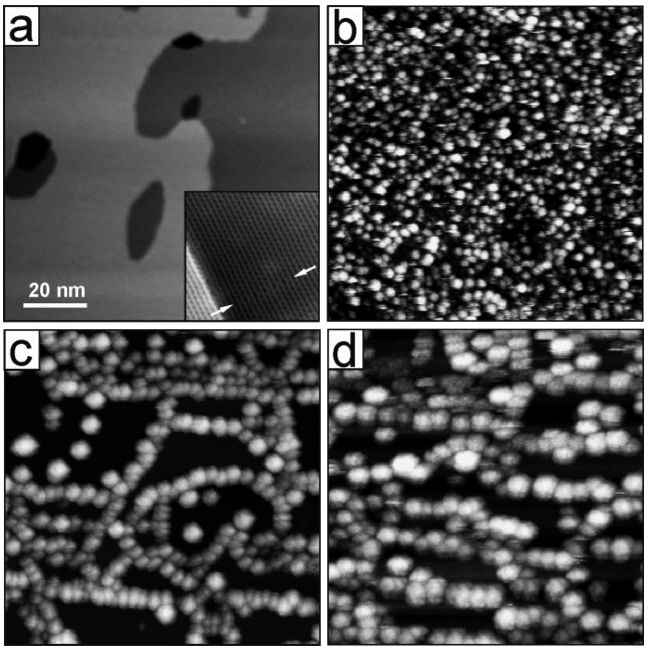

Figure 1. Room-temperature STM images of: (a) clean $SiO_{2.5}$/Mo(112) film; (b) silica nanoparticles (0.7 MLE) grown on top of the film at 100 K; (c) silica nanoparticles (0.5 MLE) grown at 300 K; all annealed in 10^{-6} mbar O_2 at 600 K. Image (d) shows the sample (c) after deposition of 0.2 ML of Au at 100 K. The scale bar shown in (a) is for all images. Inset in panel (a) shows a high-resolution image of the monolayer film, with the arrows highlighting the antiphase domain boundary.

Atomically flat terraces are separated by monatomic steps of the Mo(112) surface underneath. The orientation of the film can readily be determined through the antiphase domain boundary[13] shown in the inset.

Silica NPs were formed by Si vapor deposition in 10^{-6} mbar of O_2 and subsequent annealing at 600 K in the oxygen ambient. Room-temperature STM images of silica particles formed by the deposition at 100 and 300 K are shown in Figures 1b and 1c, respectively. In both cases, the particles exhibit a narrow size distribution. However, larger clusters only decorating step edges and domain boundary defects are formed at 300 K, whereas considerably smaller and randomly distributed particles are observed upon deposition at 100 K (NB: the sample was heated to 300 K for STM imaging). Increasing Si amounts from 0.2 MLE to 0.7 MLE at 100 K considerably increases the cluster density but only slightly the average particle size. (See Figure S1 in the Supporting Information (SI)). Table 1 summarizes structural characteristics of prepared silica NPs.

The chemical composition and the electronic structure of the samples were monitored by XPS. Figure 2 shows Si 2p spectra of NPs deposited at 300 K (a) and 100 K (b,c), all annealed at 600 K in oxygen. For NPs prepared by low-temperature deposition, only one peak is observed at 103.0 eV which is typical for the Si^{4+} oxidation state in SiO_2.[14] In contrast, NPs grown at 300 K show an additional small peak at 99.2 eV, which is indicative of metallic Si, that is quite surprising for silicon treated in oxygen at high temperatures. One may first suggest that the Si atoms migrate through the monolayer silica film in a way it has previously been reported for Pd and Ag atoms.[15] However, such a probability is strongly suppressed for the "O-rich" films[13] (solely used here) having additional O atoms only bonded to the Mo(112) surface.[16] In addition, it seems unlikely for the Si atoms interacting with the O adatoms to remain in the metallic state. Finally, such an effect should be observed for the particles prepared at 100 K as well, which is not the case. It is conceivable that the Si^0 atoms are present in the core of largest silica NPs formed at 300 K (Figure 1). It appears that enhanced surface diffusion at 300 K leads to larger aggregates which then undergo relatively slow oxidation, whereas smaller particles formed at 100 K become fully oxidized much faster. We found that additional annealing at 900 K in 10^{-6} mbar O_2 was necessary to ultimately oxidize NPs prepared at 300 K. Interestingly, STM imaging revealed that the silica NPs remain stable under this high-temperature treatment (not shown here).

In order to minimize Si migration into the film, silica NPs were also prepared using water buffer layer assisted deposition[17] as previously used for ceria nanoparticles.[5] For this, Si was deposited on top of an amorphous solid water ("ice") film covering a silica layer at 100 K and then heated to room temperature in 10^{-6} mbar of O_2. In contrast to the direct

Table 1. Structural Characteristics of Supported Silica NPs Determined by STM and Calculated Average Numbers of Au Atoms Per Silica NP[a]

sample	preparation conditions	particle density ($\times 10^{-12}$ cm^{-2})	surface area per NP[b] (in nm^2)	average NP diameter (in nm)[c]	number of Au atoms per silica NP
0.5Si-300	0.5 MLE; 300 K	3.15	8.5	4.6	32
0.2Si-100	0.2 MLE; 100 K	7.1	2.5	2.5	14
0.7Si-100	0.7 MLE; 100 K	13	1.6	2.0	7.5

[a]The error does not exceed 10%. [b]Measured using Gwyddion software (http://gwyddion.net). [c]Assuming hemispherical shape of the particles.

DOI: 10.1021/acs.jpcc.9b02592
J. Phys. Chem. C 2019, 123, 12376−12381

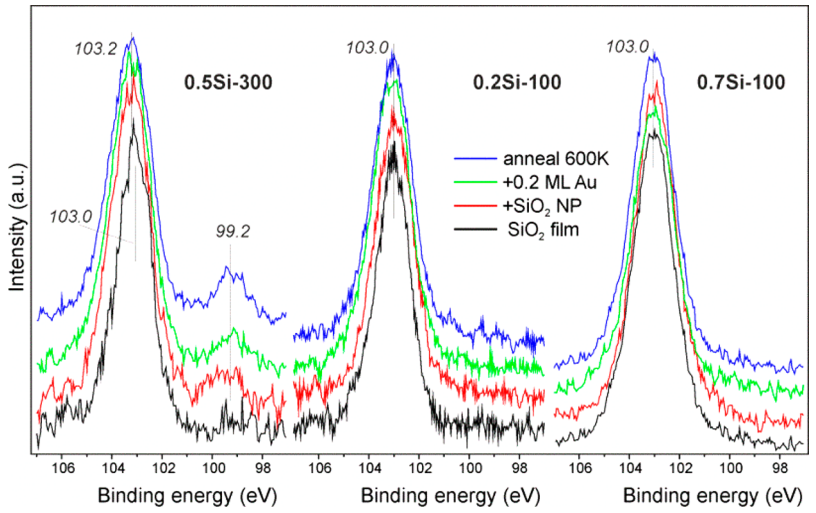

Figure 2. Si 2p XP spectra of three different samples (for labeling, see Table 1) measured after preparations as indicated. Black line corresponds to pristine silica films before silica NP deposition (in red). Au was deposited at 100 K (green) and then annealed to 600 K in UHV (blue). The spectra are offset for clarity.

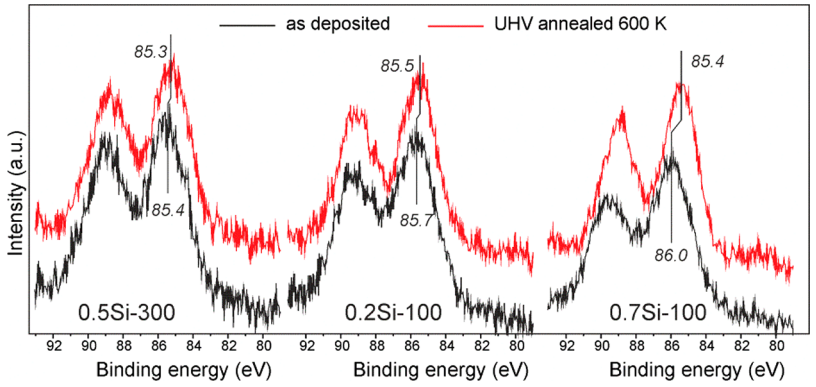

Figure 3. Au 4f region of XP spectra of 0.2 ML Au on three different silica NPs samples as indicated (for labeling, see Table 1): as deposited at 100 K (black) and after UHV annealing to 600 K (red). The spectra are offset for clarity.

Si deposition, the samples prepared by water assisted deposition showed no individual silica NPs but rather large silica islands and ill-shaped aggregates. In addition, XP spectra revealed a broad Si 2p signal between 99 and 102 eV suggesting the formation of nonstoichiometric silicon suboxides. Again, only annealing at 900 K in 10^{-6} mbar O_2 could fully oxidize silica deposits. In principle, these findings are consistent with the above-drawn conclusion that the observed Si^0 state resulted from the slow oxidation of large Si aggregates. Therefore, in the following we have only employed Si deposition on a clean silica film to prepare silica NPs.

In the next step, we studied gold interaction with different silica supports. Small amounts of gold (about 0.2 ML with respect to the Au(111) surface, or 2×10^{14} at/cm^2) were deposited at 100 K to produce highly dispersed gold and also to minimize the formation of large Au particles. Not surprisingly, for the nanosilica supports grown at 100 K (Figure 1b), it was impossible to differentiate gold and silica by STM. However, the comparison of STM images obtained on the 0.5Si-300 sample before and after gold deposition (Figure 1c,d) shows that gold does not form additional particles but increases the apparent size of existing silica NPs (although tip−sample convolution effects cannot be excluded). Note, however, that our previous STM studies[15] of gold deposited onto a monolayer silica film only showed Au particles decorating step edges and line defects, which are now occupied by silica NPs. Gold migration into the film is thermodynamically unfavorable.[16] Therefore, those Au atoms which land on the bare silica film most likely diffuse and ultimately stick to the silica NPs.

After gold deposition, the Si 2p states including the one at 99.2 eV all remain unchanged (Figure 2), even after subsequent UHV annealing at 600 K. The Au 4f spectra are shown in Figure 3. For the "as-deposited" samples at 100 K, the Au $4f_{7/2}$ peak is observed at 85.6−86.0 eV, i.e., remarkably higher than 84.0 eV on massive gold. For comparison, the spectra recorded for the same amounts of Au on the clean, NP-free silica film revealed the Au $4f_{7/2}$ state at 84.4 eV. A higher binding energy (BE) often observed for metal nanoparticles, in particular, for gold, is commonly associated with the final state effects[18] involving, for example, size-dependent screening of the core hole, thus affecting the kinetic energy of the emitted photoelectrons. As a result, the smaller the particle, the larger the BE shift to higher BEs (ΔBE). The relationship has previously been studied in detail on Pd and Rh particles deposited on alumina thin films, where it was found that ΔBE (up to 1.2 eV in this case) is inversely proportional to the mean particle size determined by STM.[19] It is expected,

DOI: 10.1021/acs.jpcc.9b02592
J. Phys. Chem. C 2019, 123, 12376−12381

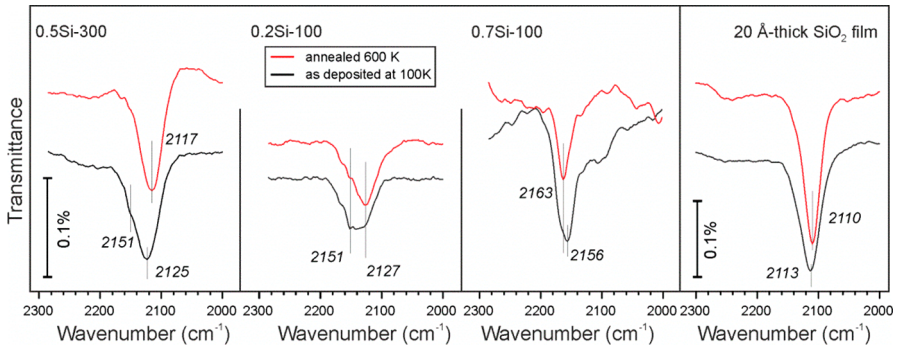

Figure 4. CO IRA spectra of 0.2 ML Au on silica NPs and a 20 Å-thick SiO_2 film: as deposited at 100 K (black lines); after annealing to 600 K (red lines). The samples were exposed to saturating amounts of CO at 100 K. No other CO related bands were observed below 2000 cm^{-1}. The spectra are offset for clarity.

however, that the $6s^1$ electronic configuration of metallic gold provides more effective screening than the D-metals like Pd and Rh, and hence the effect will be smaller. Therefore, the large ΔBE values, about 2 eV, observed here for Au on silica NPs may also be indicative of partially charged, $Au^{\delta+}$ species. Note that the $Au^{\delta+}$ formation on the Au/nano-CeO_2 system was accompanied by ceria reduction. Here, the precise state of nano-SiO_2 was difficult to monitor with XPS because of the strong signals of the silica film. However, using the Si 2p and O 1s signal intensity ratio measured for a monolayer film having the $SiO_{2.5}$ stoichiometry[12] as a reference, we estimated composition stoichiometry of silica nanoparticles to be $SiO_{2.2\pm0.2}$, although the estimation did not take into account silica morphology and attenuation factors related to the electron escape depth.

UHV annealing to 600 K shifts the Au 4f peaks to the lower BEs. In addition, the Au 4f signals become narrower, notably on the NP samples formed by low-temperature deposition. However, the BE values are still about 1 eV higher than for "bulky" gold, thus suggesting a highly dispersed state of gold even after annealing. Therefore, we can conclude that gold deposited on silica nanoparticles is thermally stable and fairly resistant toward sintering.

Luo et al.[18] studying Au deposits on amorphous silica films grown on Mo(110) also reported relatively high BEs, depending on the film thickness which varied between 3 and 50 Å (determined by attenuation of the Mo 3d signal). In addition, ion scattering results suggested gold sintering on heating from 100 to 600 K, although the Au $4f_{7/2}$ BE remained almost unchanged (85 ± 0.1 eV, at 0.2 ML Au coverage). The authors mentioned that contributions to BE shifts related to changes in roughness of the silica film with thickness and consequent higher dispersion of the Au cannot be ruled out. Our own measurements on 0.2 ML Au deposited onto an amorphous 20 Å-thick SiO_2 film prepared on Mo(112) showed 85.3 eV, i.e., in good agreement with the results of Luo et al.[18] Certainly, for "thick" insulating films, surface charging and related band bending effects play an important role for the BEs measured, which renders the precise determination of the oxidation state of Au in such systems difficult.

To shed more light on the nature of Au species on different silica supports studied, we employed IRAS spectroscopy of CO as a probe molecule commonly used for gold.[20] Figure 4 collects spectra in CO stretching region measured on Au/nano-SiO_2 samples and gold deposited onto "thick" SiO_2 film, for comparison. The spectra were measured at 100 K by exposing to 10^{-7} mbar of CO. Note that no CO adsorption at these temperatures was found on silica surfaces prior to the Au deposition.

We first address results obtained on Au deposited onto a "thick" SiO_2 film. A fairly symmetric IR band peaked at 2113 cm^{-1} is typical for CO adsorbed in on-top geometry on the metallic Au surfaces, which usually blue-shifts up to about 10 cm^{-1} when measured on small Au particles and stepped surfaces, most likely due to the coordination effect.[3] UHV annealing to 600 K leads to the band narrowing and shift to 2110 cm^{-1}, which can be assigned to gold sintering. Basically, the same behavior was previously found for Au deposited onto a monolayer silica film (2113 and 2109 cm^{-1}, respectively, before and after heating to 300 K).[5] Therefore, we may conclude that Au particles formed by vapor deposition onto extended silica films (either monolayer or 20 Å in thickness) are metallic in nature. Since XPS inspection of this sample revealed the Au $4f_{7/2}$ peak at 85.3 eV, i.e., strongly shifted, we may conclude that the observed BE shift is purely a final state effect.

When Au is deposited onto relatively large (about 5 nm, see Figure 1c) silica NPs present in the 0.5Si-300 sample, CO IR spectra showed the band at 2125 cm^{-1} with a shoulder at 2151 cm^{-1}. The latter disappears upon UHV annealing to 600 K, whereas the principal band red-shifts to 2117 cm^{-1}. For the "as-deposited" Au/0.2Si-100 sample showing much smaller silica NPs, the band at 2151 cm^{-1} even becomes comparable with the one at 2127 cm^{-1}, thus resulting in a broad signal. Again, the 2151 cm^{-1} band considerably attenuates upon UHV annealing. However, the band at 2127 cm^{-1} remains, thus indicating good thermal stability and lack of gold sintering. Although considerably shifted, the principal bands observed for the annealed samples still fall in the range of those assigned to small metallic Au particles.[3] In contrast, the band at 2151 cm^{-1} is blue-shifted with respect to the gas phase CO (2143 cm^{-1}), thus suggesting adsorption onto metal cations, hence the positively charged $Au^{\delta+}$ atoms.[20] Albeit formed at 100 K, such species are thermally unstable, as the band attenuates or even disappears on heating. However, the situation differs substantially for the Au/0.7Si-100 sample, where the spectrum is dominated by the band(s) at 2155−2163 cm^{-1} which remained after annealing to 600 K.

Note that the intensity of an IR band in IRAS depends not only on the surface density of adsorbed species but also on their orientation with respect to the metal support plane due to the well-known surface selection rules stating that only dipole moment changes normal to the metal surface are detected. Therefore, direct comparison of the samples shown in Figure 4

DOI: 10.1021/acs.jpcc.9b02592
J. Phys. Chem. C 2019, 123, 12376−12381

is not straightforward. Nonetheless, the comparison of the ν(CO) frequencies allows us to propose that the formation of thermally stable, positively charged $Au^{\delta+}$ species is favored at low Au loading (number of Au atoms per particle, see Table 1) on nanoparticulate silica supports with a small average size. It is worth noting here that our previous CO IRA spectra[5] for Au/nano-CeO_2 showed that the weak band at 2152 cm^{-1} irreversibly disappeared, while the principal 2117−2130 cm^{-1} band, observed immediately after Au deposition at 100 K, shifted to the values typical for metallic gold (2109−2112 cm^{-1}) upon annealing. This parallels the evolution of spectra observed here for the 0.5Si-300 sample (Figure 4, left panel). Taking into account similar sizes of CeO_2 particles (although prepared by water-assisted deposition) and of SiO_2 particles in these two studies, we conclude that the formation and stabilization of $Au^{\delta+}$ species depend on oxide size rather than its reducibility.

Finally, we examined the environmental stability of the Au/nano-SiO_2 systems via exposure to 3 mbar of stoichiometric (2:1) CO/O_2 mixture at 300 K. There were several studies in the literature reporting gold sintering if exposed to CO oxidation reaction conditions.[21,22] After "high-pressure" treatment, XPS spectra showed no visible contamination of the surface. However, the Au 4f lines shifted to the lower BE values, most notably for the Au/0.5Si-300 sample (from 85.3 to 84.9 eV), which are still considerably higher than on large (∼5 nm) Au nanoparticles. Interestingly, the Au/0.2Si-100 sample showed no more CO adsorption, at least at 100 K, even after further thermal flash to 600 K in UHV. In contrast, the 2165 cm^{-1} band, dominated on the Au/0.7Si-100 sample before such treatment (Figure 4), survived after CO + O_2 exposure, albeit of reduced intensity. (See Figure S2 in SI). These findings indicate that silica nanoparticles may form $Au^{\delta+}$ species that are fairly stable under CO oxidation atmosphere.

4. SUMMARY

We have studied interaction of gold with silica nanoparticles ("nano-SiO_2") prepared on an atomically flat thin silica film and characterized by STM. Combined XPS and IRAS results showed the formation of partially charged $Au^{\delta+}$ upon deposition at low temperatures on nanosilica and not on extended, both monolayer and multilayer, silica films. The results bear close similarity to what has previously been observed for gold deposited on "nano-CeO_2", prepared on the same substrate, and thin CeO_2(111) films.[5] Direct comparison of the two systems suggests that it is the nanoparticulate morphology of the oxide support rather than its reducibility that promotes the formation and stabilization of $Au^{\delta+}$ species. In the present case, it is not the increased work function of oxide that causes charge transfer (see Introduction), since its value for the $SiO_{2.5}$/Mo(112) used here as a substrate is considerably lower than for FeO/Pt(111), i.e., 4.3 eV[23] and 5.6−6.6 eV[24] (depending on the film registry), respectively. Based on experimental and theoretical results available in the literature, the possible mechanism to drive electrons from adsorbed Au into the oxide support includes a cation deficiency and/or other defects on the nanoparticle surface.

The abundance and thermal stability of $Au^{\delta+}$ species on nanosilica were found to depend on the particle size so that $Au^{\delta+}$ may dominate at the surface and be even present after UHV annealing to 600 K and exposure to the 3 mbar of the CO + O_2 mixture at 300 K. As the "cationic" gold in supported catalysts is believed to play an important role in the CO oxidation and water−gas shift reactions,[25,26] the results may open new routes in synthesis of efficient silica-supported gold catalysts.

■ ASSOCIATED CONTENT

Supporting Information

The Supporting Information is available free of charge on the ACS Publications website at DOI: 10.1021/acs.jpcc.9b02592.

STM-based size distribution of silica nanoparticles and IRA spectra of the samples treated at CO + O_2 reaction mixtures in the mbar pressure range (PDF)

■ AUTHOR INFORMATION

Corresponding Author

*E-mail: shaikhutdinov@fhi-berlin.mpg.de.

ORCID

Oleksandr Bondarchuk: 0000-0001-7380-8930
Shamil Shaikhutdinov: 0000-0001-9612-9949
Hans-Joachim Freund: 0000-0001-5188-852X

Present Address

#International Iberian Nanotechnology Laboratory, Av. Mestre José Veiga, s/n4715-330 Braga, Portugal.

Notes

The authors declare no competing financial interest.

■ ACKNOWLEDGMENTS

The work was supported by the Fonds der Chemischen Industrie.

■ REFERENCES

(1) Haruta, M. When Gold Is Not Noble: Catalysis by Nanoparticles. *Chem. Rec.* **2003**, *3*, 75−87.

(2) *Gold Nanoparticles for Physics, Chemistry and Biology*, 2nd ed.; Louis, C., Pluchery, O., Eds.; World Scientific Publishing Europe Ltd.: NJ, 2017.

(3) Meyer, R.; Lemire, C.; Shaikhutdinov, S. K.; Freund, H. J. Surface Chemistry of Catalysis by Gold. *Gold Bull.* **2004**, *37*, 72−124.

(4) Wang, A.; Li, J.; Zhang, T. Heterogeneous Single-atom Catalysis. *Nature Rev. Chem.* **2018**, *2*, 65−81.

(5) Baron, M.; Bondarchuk, O.; Stacchiola, D.; Shaikhutdinov, S.; Freund, H. J. Interaction of Gold with Cerium Oxide Supports: CeO_2(111) Thin Films vs CeO_x Nanoparticles. *J. Phys. Chem. C* **2009**, *113*, 6042−6049.

(6) Carrettin, S.; Concepcion, P.; Corma, A.; Nieto, J. M. L.; Puntes, V. F. Nanocrystalline CeO_2 Increases the Activity of Au for CO Oxidation by Two Orders of Magnitude. *Angew. Chem., Int. Ed.* **2004**, *43*, 2538−2540.

(7) Pan, Y.; Nilius, N.; Freund, H.-J.; Paier, J.; Penschke, C.; Sauer, J. Titration of Ce^{3+} Ions in the CeO_2(111) Surface by Au Adatoms. *Phys. Rev. Lett.* **2013**, *111*, 206101.

(8) Giordano, L.; Pacchioni, G.; Goniakowski, J.; Nilius, N.; Rienks, E. D. L.; Freund, H.-J. Charging of Metal Adatoms on Ultrathin Oxide Films: Au and Pd on FeO(111)/Pt(111). *Phys. Rev. Lett.* **2008**, *101*, 026102.

(9) Sterrer, M.; Risse, T.; Martinez Pozzoni, U.; Giordano, L.; Heyde, M.; Rust, H.-P.; Pacchioni, G.; Freund, H.-J. Control of the Charge State of Metal Atoms on Thin MgO Films. *Phys. Rev. Lett.* **2007**, *98*, 096107.

(10) Chang, M.-W.; Sheu, W.-S. The Charge States of Au on Gold-substituted $Ce_{1-x}O_2$(111) Surfaces with Multiple Oxygen Vacancies. *Phys. Chem. Chem. Phys.* **2016**, *18*, 15884−15893.

(11) Brown, M. A.; Ringleb, F.; Fujimori, Y.; Sterrer, M.; Freund, H.-J.; Preda, G.; Pacchioni, G. Initial Formation of Positively Charged Gold on MgO(001) Thin Films: Identification by Experiment and

DOI: 10.1021/acs.jpcc.9b02592
J. Phys. Chem. C 2019, 123, 12376−12381

Structural Assignment by Theory. *J. Phys. Chem. C* **2011**, *115*, 10114−10124.
(12) Weissenrieder, J.; Kaya, S.; Lu, J. L.; Gao, H. J.; Shaikhutdinov, S.; Freund, H. J.; Sierka, M.; Todorova, T. K.; Sauer, J. Atomic Structure of a Thin Silica Film on a Mo(112) Substrate: A Two-Dimensional Network of SiO_4 Tetrahedra. *Phys. Rev. Lett.* **2005**, *95*, 076103.
(13) Todorova, T. K.; Sierka, M.; Sauer, J.; Kaya, S.; Weissenrieder, J.; Lu, J. L.; Gao, H. J.; Shaikhutdinov, S.; Freund, H. J. Atomic Structure of a Thin Silica film on a Mo(112) Substrate: A Combined Experimental and Theoretical Study. *Phys. Rev. B: Condens. Matter Mater. Phys.* **2006**, *73*, 165414.
(14) Himpsel, F. J.; McFeely, F. R.; Taleb-Ibrahimi, A.; Yarmoff, J. A.; Hollinger, G. Microscopic Structure of the SiO_2/Si Interface. *Phys. Rev. B: Condens. Matter Mater. Phys.* **1988**, *38*, 6084−6096.
(15) Ulrich, S.; Nilius, N.; Freund, H.-J.; Martinez, U.; Giordano, L.; Pacchioni, G. Realization of an Atomic Sieve: Silica on Mo(112). *Surf. Sci.* **2009**, *603*, 1145−1149.
(16) Baron, M.; Stacchiola, D.; Ulrich, S.; Nilius, N.; Shaikhutdinov, S.; Freund, H. J.; Martinez, U.; Giordano, L.; Pacchioni, G. Adsorption of Au and Pd Atoms on Thin SiO_2 Films: the Role of Atomic Structure. *J. Phys. Chem. C* **2008**, *112*, 3405−3409.
(17) Gross, E.; Asscher, M.; Lundwall, M.; Goodman, D. W. Gold Nanoclusters Deposited on SiO_2 via Water as Buffer Layer: CO-IRAS and TPD Characterization. *J. Phys. Chem. C* **2007**, *111*, 16197−16201.
(18) Luo, K.; Kim, D. Y.; Goodman, D. W. The Nucleation and Growth of Gold on Silica. *J. Mol. Catal. A: Chem.* **2001**, *167*, 191−198.
(19) Bäumer, M.; Freund, H.-J. Metal Deposits on Well-ordered Oxide Films. *Prog. Surf. Sci.* **1999**, *61*, 127−198.
(20) Mihaylov, M.; Knözinger, H.; Hadjiivanov, K.; Gates, B. C. Characterization of the Oxidation States of Supported Gold Species by IR Spectroscopy of Adsorbed CO. *Chem. Ing. Tech.* **2007**, *79*, 795−806.
(21) Lu, J. L.; Gao, H. J.; Shaikhutdinov, S.; Freund, H. J. Gold Supported on Well-ordered Ceria Films: Nucleation, Growth and Morphology in CO Oxidation Reaction. *Catal. Lett.* **2007**, *114*, 8−16.
(22) Kolmakov, A.; Goodman, D. W. Scanning Tunneling Microscopy of Gold Clusters on TiO_2(110): CO Oxidation at Elevated Pressures. *Surf. Sci.* **2001**, *490*, L597−L601.
(23) Lichtenstein, L.; Heyde, M.; Ulrich, S.; Nilius, N.; Freund, H.-J. Probing the Properties of Metal−Oxide Interfaces: Silica Films on Mo and Ru supports. *J. Phys.: Condens. Matter* **2012**, *24*, 354010.
(24) Giordano, L.; Pacchioni, G.; Goniakowski, J.; Nilius, N.; Rienks, E. D. L.; Freund, H.-J. Interplay Between Structural, Magnetic, and Electronic Properties in a FeO/Pt(111) Ultrathin Film. *Phys. Rev. B: Condens. Matter Mater. Phys.* **2007**, *76*, 075416.
(25) Wang, X.; Chen, B.; Chen, G.; Sun, X. Oxygen Vacancies Dependent Au Nanoparticle Deposition and CO Oxidation. *RSC Adv.* **2016**, *6*, 87978−87987.
(26) Deng, W.; Frenkel, A. I.; Si, R.; Flytzani-Stephanopoulos, M. Reaction-Relevant Gold Structures in the Low Temperature Water-Gas Shift Reaction on Au-CeO_2. *J. Phys. Chem. C* **2008**, *112*, 12834−12840.

DOI: 10.1021/acs.jpcc.9b02592
J. Phys. Chem. C 2019, 123, 12376−12381